MSDE

PAPER

Cite this: *Mol. Syst. Des. Eng.*, 2020, **5**, 1003

Theoretical evaluation of hexazinane as a basic component of nitrogen-rich energetic onium salts†

Sergey V. Bondarchuk

Received 22nd January 2020,
Accepted 14th May 2020

DOI: 10.1039/d0me00007h

rsc.li/molecular-engineering

In the present paper, we report a comprehensive theoretical evaluation of a hypothetical compound, hexazinane (*cyclo*-H_6N_6), and its 10 onium salts as high-energy density materials. Crystal structure prediction, which included dynamical and mechanical stability criteria estimation, found a $P2_1/c$ space group crystal structure to be the lowest energy polymorph. Prediction of the chemical reactivity parameters of a hexazinane molecule revealed a strong basic character comparable with those of secondary and tertiary aliphatic amines. The onium salts of hexazinane with the carbon-free inorganic anions $(N_xO_y)^-$ and with several low carbon content organic anions demonstrate excellent detonation characteristics. Hexazinanium nitrate $H_7N_6^+NO_3^-$ has detonation performance comparable with ε-CL-20, the most powerful non-nuclear explosive known. The corresponding salts with dinitramide $N(NO_2)_2^-$ and nitrite NO_2^- anions have only slightly lower characteristics more powerful than all known explosives, except for ε-CL-20 and octanitrocubane. The reported "green" energetic materials also demonstrate excellent propulsive performance, and, if synthesized, these may find potential applications as solid rocket propellants.

Design, System, Application

Crystal structure prediction is the most accurate method for the theoretical design of novel energetic materials, and outperforms simple molecular predictions with respect to estimation of the material's density, enthalpy of formation and stability of the solid phase. The current manuscript utilizes state-of-the-art computational techniques as well as a new strategy for the prediction of molecular crystals. Hexazinane is an excellent candidate for energetic materials due to its high energy density, nitrogen content and nucleophilicity. The synthesis of hexazinane and its ammonium salts may provide the most powerful non-nuclear weapon. Calculations predict a set of carbon-free salts of hexazinane to have the highest detonation and propulsive properties among the known energetic materials, whereas the main detonation products will be molecular nitrogen and water.

Introduction

Besides one theoretical study of H_6N_6 isomers[1] and the provocative book of the controversial author Jared Ledgard,[2] only two databases, PubChem[3] and Mol-Instincts,[4] mention hexazinane (*cyclo*-H_6N_6) or its derivatives as possible chemical compounds. This substance was proposed earlier as a potential explosive agent in the form of 1,3,5-trinitro, 1,3,5-triazido derivatives and trisodium hexazinane-1,3,5-triide.[2] The book even offers detailed methods for the preparation of these compounds, although the validity of the latter is highly doubtful, since the book does not contain any relevant references. Nevertheless, despite the absurdity of many statements and approaches in this book, the idea itself about the use of hexazinane as a potential high-energy density material (HEDM) can scarcely be considered the same, since hexazinane has a much higher energy density compared to its linear isomers.[1]

Indeed, *cyclo*-H_6N_6 has all chances to be synthesized. In the molecular form, the nitrogen cycle exists in the armchair conformation, which allows reducing of internal strain present in triaziridine[5–7] or other three-membered nitrogen cycles.[8] The lone pairs of the sp^3 hybridized nitrogen atoms are directed so that the energetically unfavorable overlap is minimal. Finally, the nitrogen and hydrogen atoms form simple covalent N–N and N–H bonds, like in hydrazine, while in the condensed phase, additional stabilization comes from the N···H hydrogen bonds. All these factors suggest the possible thermodynamic stability of the molecule; however,

Department of Chemistry and Nanomaterials Science, Bogdan Khmelnitsky Cherkasy National University, Blvd. Shevchenko 81, 18031 Cherkasy, Ukraine. E-mail: bondchem@cdu.edu.ua

† Electronic supplementary information (ESI) available: Crystal packing, fractional coordinates, crystal habit parameters, elastic constants, vibrational spectra, thermodynamic data, coefficients of the NASA polynomials and equilibrium composition of exhaust gases. See DOI: 10.1039/d0me00007h

the final verdict should obviously come from its chemical and thermal stability.

Considering the structure of hexazinane (*n*-nucleophile), the most probable role of this compound in a HEDM is to be a basic component of onium energetic salts. Indeed, such salts are known for a wide variety of nitrogen-rich heterocyclic compounds.[9–13] These are generally characterized by low sensitivity and high detonation performance.[14,15] Moreover, nitrogen-rich salts are environmentally friendly energetic materials, since the main detonation product is molecular nitrogen N_2. Thus, taking into account millions of tons of explosives applied per year in the world, a large amount of carbon oxides is released into the atmosphere facilitating the greenhouse effect. As a result, carbon-free nitrogen-rich energetic compounds are of special interest since they produce mostly N_2 and H_2O as the detonation products.

In this context, carbon-free $H_xN_yO_z$ energetic salts are usually a combination of the following anions and cations: NH_4^+, N_2H–NH_3^+, HO–NH_3^+, N_3^-, *cyclo*-N_5^-, $N(NO_2)_2^-$, and NO_3^-.[15–19] It is obvious that not all the ions are energetic. For example, the NH_4^+ cation has a negative enthalpy of formation (−132.8 kJ mol^{-1})[20] and replacement of this basic component in the above-mentioned salts by one with a high positive enthalpy of formation will significantly increase detonation characteristics. Therefore, we have tried to model hexazinane salts with the above-mentioned anions as well as with some widely used carbon-containing anions in order to check their detonation and propulsive performances.

For this purpose, we have predict the crystal structure of parent hexazinane and its salts using evolutionary algorithm USPEX.[21] This method was effectively applied earlier to perform the crystal structure prediction of $NH_4^+N_5^-$.[22] And though the space group was determined incorrectly (*Pbcm* instead of *Pcca*), the obtained arrangement of ions in the crystal was really close to the one experimentally obtained.[16]

Computational details

In this work, crystal structure predictions were performed using both the Universal Structure Predictor: Evolutionary Xtallography (USPEX)[21] and Polymorph[23] codes. In the USPEX calculations, input structures were generated using the algorithm described in ref. 24. The value of the initial population size was specified to be 100. The latter are randomly generated structures, while the next 29 generations included 50 structures each and these 50 structures were partitioned according to the following variation operators applied: fracGene (50%), fracRand (30%), fracAtomsMut (10%) and fracRotMut (10%). As a total energy code for structure relaxation, we have applied the Density Functional based Tight Binding method (DFTB+, version 19.1)[25] The second-order energy expression involving self-consistent charge (SCC-DFTB) approximation with the Slater–Koster library 3OB[26] and with the Lennard-Jones empirical correction for van der Waals interactions was applied.

For the Polymorph calculations, molecules and ions were first optimized using the DFT(B3LYP)/6-311++G(2d,2p) method[27,28] and their Merz–Kollman electrostatic potential fitting partial charges were obtained. These calculations were done using the Gaussian09 program package.[29] The obtained charges were applied further within the structure prediction with the Polymorph code. At the packing step, a simulated annealing procedure was performed, during which thousands of crystal structures were built and randomly modified. The clustering step proceeded until all available frames for the specified space groups were clustered. For the geometry optimization step we have applied Condensed-phase Optimized Molecular Potentials for Atomistic Simulation Studies (COMPASS) force field.[30] Rigid body constraints were specified for molecules and ions; thus, the B3LYP optimized geometries were utilized at this step.

The crystal structures obtained with the USPEX and Polymorph calculations were then completely relaxed with the Cambridge Serial Total Energy Package (CASTEP) code[31] implemented in the Materials Studio 7.0 program suite.[32] Norm-conserving (NC) pseudopotentials and the functional due to Perdew–Burke–Ernzerhof (PBE)[33] were applied entirely. Wave functions were expanded in a plane wave basis set with an energy cutoff of 830 eV (61.0 Ry). Sampling of the Brillouin zones was performed using *k*-point grids generated by the Monkhorst–Pack algorithm. The direct spacing between *k*-points was specified to be 0.08 2π Å^{-1} for all the cell relaxations. The convergence criterion of the total energy was set to 5×10^{-6} eV per atom. Dispersion effects were taken into account (in the CASTEP and DMol^3 calculations) by means of the Grimme form of the damped C_6 term.[34]

Frequency analyses were then performed using the DMol^3 code.[35] For this purpose, all the crystals were relaxed again using the all-electron approximation along with the PBE functional and the triple numerical basis set TNP.[35] Note that energies obtained with these calculations were then applied for estimations of sublimation enthalpies. DMol^3 cannot produce the second derivatives analytically; thus, a finite difference approximation is applied to the first derivatives. Within this approach, the second derivatives are computed numerically using eqn (1).[35]

$$\frac{\partial^2 E}{\partial q_i \partial; q_j} \equiv \left[\frac{\partial}{\partial q_i} E\left(q_j + \Delta\right) - \frac{\partial}{\partial q_i} E\left(q_j\right)\right] / \Delta, \quad (1)$$

where Δ is an arbitrary distance by which the equilibrium geometry is displaced.

Results and discussion

Crystal structure, stability criteria and reactivity parameters of hexazinane

Since the hexazinane ring is built from the sp^3 hybridized nitrogen atoms, it exists in the most thermodynamically stable chair conformation, like in cyclohexane. However, the most preferable equatorial positions of hydrogens in the latter compound become absolutely unfavorable in

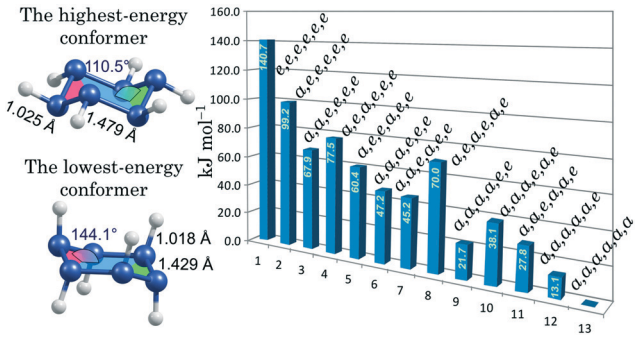

Fig. 1 The calculated energies of the hexazinane chair conformers.

hexazinane. As one can see in Fig. 1, the most energetically preferable conformer corresponds to the *a*,*a*,*a*,*a*,*a*,*a* positions of the hydrogen atoms and the energy difference between marginal conformers exceeds 140 kJ mol^{-1}. This situation is similar to the 1,4,2,3,5,6-dioxatetrazinane molecule, another very powerful green explosive, which is studied in our laboratory.[36] It is interesting that bond lengths and torsion angles are quite different in the equatorial and axial conformers. In the *a*,*a*,*a*,*a*,*a*,*a* conformer, the N–N and N–H bonds are shorter meaning that the molecule is more robust mechanically.

Thus, the latter conformer was used for the crystal structure prediction. In the USPEX calculations we have applied 4 runs with different Z' values (1 to 4). The predicted crystal structures are illustrated in Fig. 2, and correspond to the following Z' values: $C2/m$ (Z' = 1), $P2_1/c$ (Z' = 2) and *Cmca* (Z' = 4). Despite the hexazinane molecule having the D_{3d} point group symmetry, none of the predicted crystals has a third order axis. In contrast, a mirror plane was found in two crystals (Fig. 2). In the case of Z' = 3, the calculation gives a $P1$ space group structure being significantly higher in energy and not discussed herein. The corresponding crystal packing is illustrated in Fig. S1 in the ESI.† Along with these calculations, we have applied our modified eigenvector-following scheme[37] to perform the crystal structure prediction of the highest-energy conformer *e*,*e*,*e*,*e*,*e*,*e*. The calculations give a crystal structure with the space group $R\bar{3}$ (Z' = 1) (Fig. S2 in the ESI†) with a relative enthalpy of formation +85.3 kJ mol^{-1}. The fractional coordinates of the symmetry-unique atoms in the predicted crystals are listed in Table S1 in the ESI.†

Additionally, we have determined crystal morphologies in a vacuum using the attachment energy method,[38] which was found to be reliable for a number of compounds, including nitrogen-rich bistetrazole-based energetic salts.[39] The corresponding crystal habits are illustrated in Fig. 2. In all the cases, the crystals have prismatic habits with two unique faces. The numerical data on the habits' properties including face multiplicity, growth slice thickness (d_{hkl}) and relative facet areas are listed in Table S2 in the ESI.† In the case of the $P2_1/c$ crystal, the habit has a plate-like shape with the biggest aspect ratio. Of course, the growth morphology is dependent on the solvent[40] and, if synthesized, the crystal habits may be somewhat different. However, as one can see in Fig. S3 in the ESI,† the corresponding Connolly surfaces are rather flat that disfavors the solvent adsorption and weakens its influence.[40] Conversely, the other two habits (especially the *Cmca* crystal) are expected to be strongly solvent-dependent.

To justify the predicted crystal structures as stable ones at ambient pressure, we have performed calculations of their dynamical and mechanical stability. The corresponding Born–Huang criteria[41] along with the Brillouin zone integration paths in terms of the high-throughput approximation[42] are presented in Fig. S4 in the ESI.† The obtained phonon dispersions are illustrated in Fig. 3. These

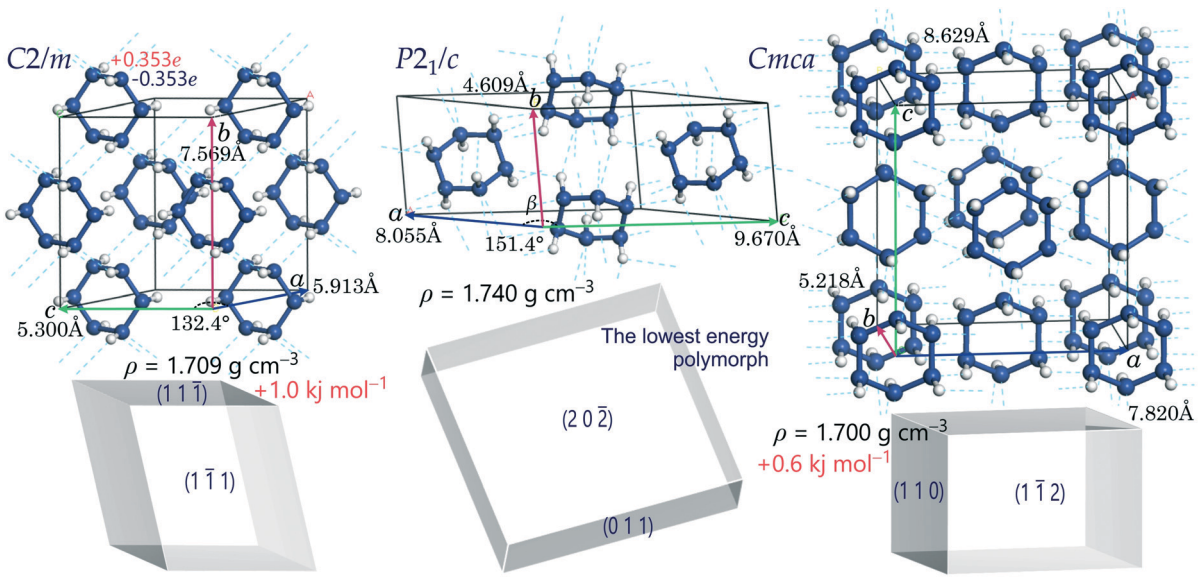

Fig. 2 Crystal structure of the three most stable polymorphs of hexazinane predicted at ambient pressure.

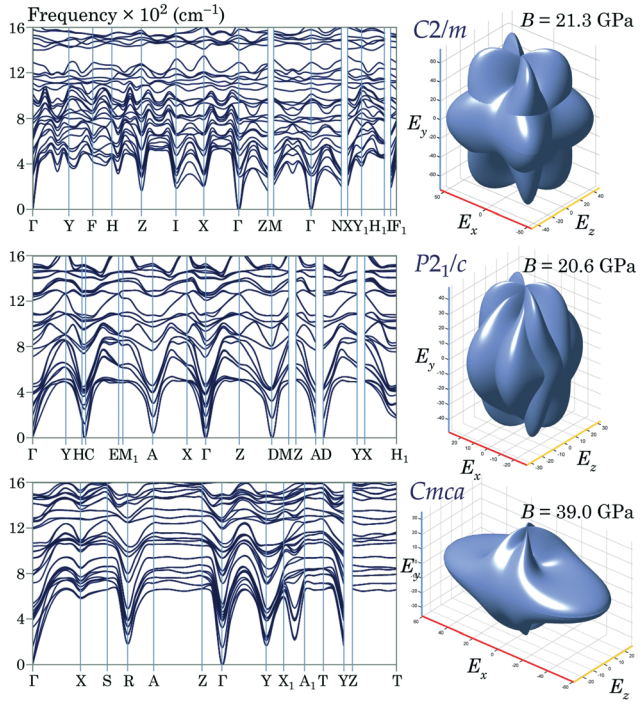

Fig. 3 Zero-pressure phonon dispersion and 3D presentation of the Young's modulus.

are characterized by the complete absence of soft modes inside the entire Brillouin zone indicating the dynamical stability. Moreover, the analysis of the calculated elastic stiffness constants C_{ij} (Table S3 in the ESI†) indicated the mechanical stability of all the three polymorphs. The obtained 3D-surfaces of the Young's modulus are illustrated in Fig. 3. Thus, the predicted polymorphs are robust crystalline materials, stable at ambient pressure. Note that the high-energy polymorph *e*,*e*,*e*,*e*,*e*,*e* is also predicted to be dynamically and mechanically stable (Fig. S5 in the ESI†). The calculated infrared (IR) spectra along with the temperature dependence of the main thermodynamic functions for the four hexazinane polymorphs are presented in Fig. S6 in the ESI.†

As follows from Fig. 2, the $P2_1/c$ crystal is the lowest energy polymorph. Thus, all further discussion will be concerned with this crystal. It is interesting to estimate chemical properties of hexazinane as a pure substance. Obviously, this molecule is an *n*-nucleophile, like ammonia or amines. But what is the performance of hexazinane compared to those of various well-known nucleophiles? In Table 1, we have gathered several calculated parameters of chemical reactivity, namely, proton affinity (PA, kJ mol^{-1}), adiabatic ionization energy (IE, eV) and electron affinity (EA, eV), as well as electrophilicity index[43] (ω, eV) and nucleophilicity index[44] (N, eV). The latter two quantities are calculated according to eqn (2) and (3).

Table 1 Parameters of chemical reactivity calculated using DFT and available experimental values in parentheses

Entry	PA		IE		EA	ω	N
H_6N_6	901.2		6.93		−0.48	0.70	4.34
NH_3	844.2	(853.6)	10.19	(10.07)	−0.69	1.04	1.08
CH_3NH_2	891.5	(899.0)	8.91	(8.90)	−0.63	0.90	2.36
$(CH_3)_2NH$	921.4	(929.5)	8.14	(8.24)	−0.61	0.81	3.13
NH_2NH_2	855.8	(853.2)	7.93	(8.10)	−0.66	0.77	3.34
NH_2OH	805.7		9.16	(10.00)	−0.72	0.90	2.11

$$\omega = \frac{(\mathrm{IE}+\mathrm{EA})^2}{8(\mathrm{IE}-\mathrm{EA})} \quad (2)$$

$$N = \mathrm{IE}_{\mathrm{TCE}} - \mathrm{IE}_{\mathrm{Nu}}, \quad (3)$$

where subscript TCE stands for tetracyanoethylene ($\mathrm{IE}_{\mathrm{TCE}}$ = 11.27 eV) as a reference. In this approach, the nucleophilicity index for TCE is zero, presenting the highest ionization energy in a long series of organic molecules already considered.[44]

As follows from Table 1, hexazinane has the highest PA after dimethylamine and the highest EA values. At the same time, this molecule possesses the highest N value. Thus, we can safely conclude that hexazinane is a very strong nucleophile comparable with secondary and tertiary aliphatic amines. Such chemical reactivity of hexazinane makes this molecule to be an effective basic component of various onium salts. We should stress that our calculated results in Table 1 are in an excellent agreement with the available experimental data taken from the NIST database.[45]

Since hexazinane has an energetic structural motif, a six-membered nitrogen ring, it is important to know its standard enthalpy of formation in solid state to estimate its detonation and propulsive characteristics. For this purpose, we have applied a two-step scheme which assumes the calculation of the gas phase enthalpy of formation and the lattice energy. Both these quantities are then used to calculate the solid-state enthalpy of formation. Thus, the first step assumes the calculation of the gas-phase enthalpy of formation ΔH_{gas} (eqn (4)).[46]

$$\Delta H_{\mathrm{gas}} = E_{\mathrm{C}_i\mathrm{H}_j\mathrm{N}_k\mathrm{O}_l\mathrm{Cl}_m} - (iE_{\mathrm{C}} + jE_{\mathrm{H}} + kE_{\mathrm{N}} + lE_{\mathrm{O}} + mE_{\mathrm{Cl}}) \quad (4)$$

where $E_{\mathrm{C}_i\mathrm{H}_j\mathrm{N}_k\mathrm{O}_l\mathrm{Cl}_m}$ and E_X are the ZPE corrected total energies of the given molecule and the constituting elements in their stationary states (graphite, $^1\Sigma_g^+$ H_2, $^1\Sigma_g^+$ N_2, $^3\Sigma_g^-$ O_2 and $^1\Sigma_g^+$ Cl_2). At the B3LYP/6-311++G(2d,2p) level of theory, these values are the following: E_{C} = −38.12160, E_{H} = −0.58498, E_{N} = −54.77927, E_{O} = −75.18198 and E_{Cl} = −460.20999 Ha. These energies are slightly modified in order to obtain the best fit with the standard gas-phase enthalpies of formation of twenty C–H–N–O–Cl compounds of different families (Table S4 in the ESI†).

The next step is the calculation of the sublimation enthalpy (ΔH_{sub}), for which the lattice energy (E_{latt}) is required (eqn (5)):

$$\Delta H_{\mathrm{sub}} = -E_{\mathrm{latt}} - 2RT = -\frac{E_{\mathrm{solid}}}{Z'} + E_{\mathrm{gas}} - 2RT, \quad (5)$$

where E_{solid} and E_{gas} are the energies of an asymmetric cell and an isolated molecule, respectively; Z' is the number of formula units per asymmetric cell. Finally, the solid-state enthalpy of formation ΔH_{solid} can be easily obtained using eqn (6).

$$\Delta H^0_{solid} = \Delta H^0_{gas} - \Delta H_{sub} \quad (6)$$

We have also checked how this approach reproduces the known solid state enthalpies of formation for the three crystalline salts (Table S5 in the ESI†). It is interesting that the reported value of ΔH_{solid} for TKX-50 determined experimentally on the basis of bomb calorimetry measurements is 473 kJ mol^{-1}.[47] Actually, we have been very surprised to obtain the value which is more than three times lower and equals 115.9 kJ mol^{-1} (Table S5 in the ESI†). However, after a careful literature review, we have found that another group of researchers also faced with this problem.[48] In their experiment, the ΔH_{solid} value for TKX-50 was found to be 114.0 kJ mol^{-1} being very close to the one calculated in the present work. Thus, we can conclude that our theoretical approach is reliable and accurate.

Using the above-described approach, the calculated enthalpies for hexazinane are the following: ΔH_{gas} = 608.9 kJ mol^{-1}, ΔH_{sub} = 169.2 kJ mol^{-1} and ΔH_{solid} = 439.7 kJ mol^{-1}. The latter value reveals a high energy density of hexazinane, which is expected to be an effective energetic material itself. But, it is more interesting to study the onium salts of hexazinane with other energetic (acidic) components, which can improve the strongly negative oxygen balance of pure hexazinane, increase its detonation properties and, at the same time, decrease sensitivity due to the formation of salts.

Detonation and propulsive performance of the nitrogen-rich onium salts of hexazinane

In this section we describe our crystal structure prediction and characterization of the 10 onium salts of hexazinane as high-energy density materials. Since we are focused mainly on the study of carbon-free salts, we have used all known anions $H_xN_yO_z$, which are already used in such salts. Additionally, we have chosen several nitrogen- and oxygen-rich anions with a small amount of carbon. Salts formed this way have improved oxygen balance and higher densities due to more strong hydrogen bonds formed.

The optimized asymmetric cells of salts **1–10** are illustrated in Fig. 4 and the lattice parameters are listed in Table 2. For the crystal structure prediction, we have combined the features of two popular predictors, USPEX and Polymorph, since both have own advantages and drawbacks. The main drawback of the Polymorph predictor is that the space group must be defined manually. This often may become critical for prediction. On the other hand, USPEX also has a disadvantage which allows trapping on another potential energy surface, which corresponds to a more stable composition. In both cases, crystal structures obtained this way will be wrong.

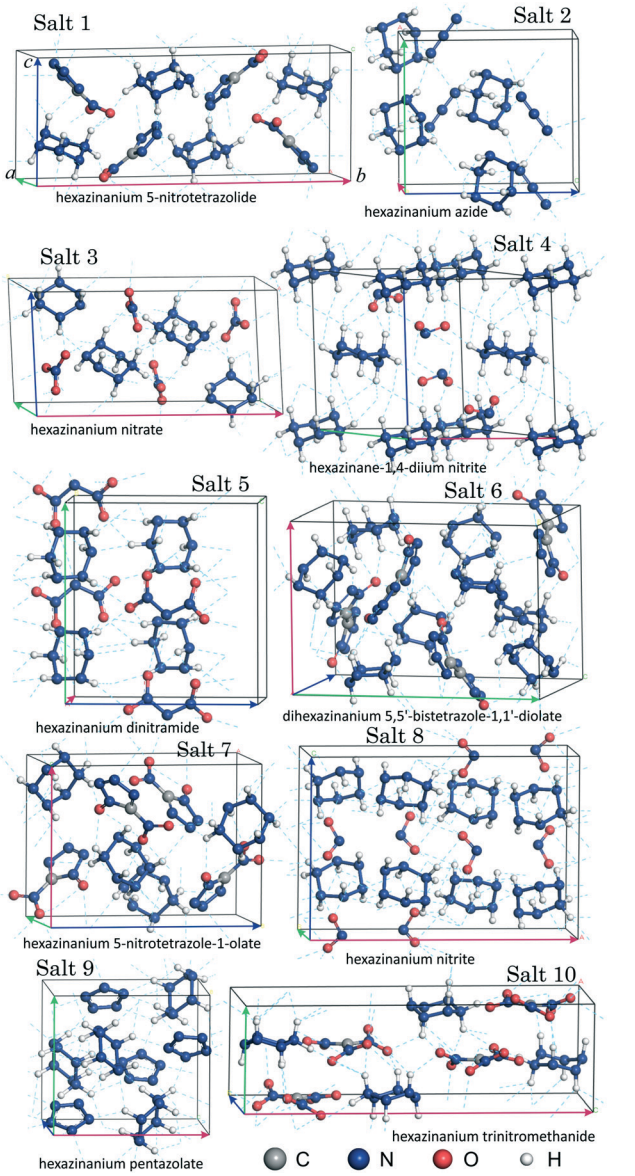

Fig. 4 Predicted crystal structures of ten hexazinane onium salts with nitrogen-rich anions (dotted lines indicate auto-detected hydrogen bonds).

Table 2 The optimized lattice parameters and space groups of salts **1–10**

Salt	SG	*a*	*b*	*c*	*β*
1	$P2_1/c$	5.267	18.426	7.372	90.6
2	$Pna2_1$	8.880	6.044	9.555	
3	$P2_1/c$	4.972	15.163	7.442	72.4
4	$P2_1/c$	8.495	8.936	7.545	142.8
5	$Pna2_1$	10.804	6.289	10.354	
6	$P2_12_12_1$	14.121	9.696	9.413	
7	$P2_12_12_1$	7.707	8.848	11.612	
8	$Pbca$	15.560	6.083	10.645	
9	$P2_12_12_1$	8.805	7.918	8.550	
10	$Pna2_1$	6.178	19.811	7.014	

Therefore, we have developed the following computational algorithm. First of all, we have performed a set of USPEX calculations with $Z' = 2$ and $Z' = 4$ as the most probable. In this case, crystal systems up to orthorhombic (space groups 2–74) were allowed for construction as initial structures. More symmetric crystal systems are too implausible for such salts and scarcely occur in reality. As a result of the USPEX calculations, the most probable space groups for salts **1–10** were determined. It is interesting that all these space groups show hits in the seven most frequent space groups, which cover 84.5% of all organic and organometallic crystal structures in the Cambridge Structural Database.[49]

Thereafter, the crystal structures of salts **1–10** were predicted using the Polymorph predictor. In this case, we have performed prediction for all these 7 most frequent space groups, which are the following: $P2_1/c$ (34.4%), $P\bar{1}$ (24.9%), $C2/c$ (8.3%), $P2_12_12_1$ (7.1%), $P2_1$ (5.1%), $Pbca$ (3.3%) and $Pna2_1$ (1.4%).[49] The lowest energy crystals were used for further calculations. The relative energies of all the predicted crystal structures are gathered in Table S6 in the ESI.† Thus, as one can see in Table 2, salts **1**, **3** and **4** belong to the monoclinic crystal system and the other salts show hits in the orthorhombic crystal system. Moreover, due to the high-symmetry positions of cations and anions in salt **4**, the crystal corresponds to $Z' = 2$, which is relatively rare for the $P2_1/c$ space group, for which $Z' = 4$ is the most frequent.[50] Note that the space groups of salts **1**, **3**, **4** and **9** are different in Table S6.† This is because the predicted lowest energy structures of these salts appeared to have imaginary frequencies in the vibrational spectra. Thus, the next polymorph in each series was optimized using first-principles calculations and its IR spectrum was analyzed. This is probably ascribed to the artifacts of the COMPASS forcefield applied within the Polymorph predictions.

All these crystals were checked for the absence of imaginary frequencies at the Γ-point only; see Table 3 for the numerical values of ν_1 (in cm^{-1}) and Fig. S7† for the whole spectral plots. As follows from Table 3, all the crystals demonstrate the complete absence of imaginary frequencies. Of course, one needs to perform phonon dispersion calculations to prove the dynamical stability of these crystals, but since this is a very expensive procedure, we have omitted this step, being satisfied with the results described above. We should stress that even very sophisticated methods or advanced procedures do not guarantee that the predicted crystal structures will reflect the true nature-created crystals. Sometimes it happens, but sometimes it does not. Therefore, one should clearly understand how strongly the predicted crystal properties are polymorph-dependent.

Fortunately, the two parameters we need to predict are the crystal density and solid-state enthalpy of formation and both these quantities are usually very well-reproduced. Moreover, for the majority of organic crystals, the energy separation between polymorphs does not exceed 2 kJ mol^{-1} and the average difference between their densities is about 0–2%.[51] We have recently obtained similar results for the crystal structure prediction of benzene diazonium chloride with the Polymorph predictor.[52] Thus, such small deviations between polymorphs do not cause significant influence on the detonation properties and this difference can be simply dropped.

As one can see in Table 3, all salts have very high solid-state enthalpies of formation, which means the high energy density of these crystals. The finite size models used for the gas phase enthalpy of formation and lattice energy calculations for salts **1–10** are illustrated in Fig. S8 in the ESI.† Taking into account relatively high crystal densities (Table 4), salts **1–10** and pure hexazinane itself are very good candidates for novel high-performance energetic salts. For the calculation of the detonation properties, namely, detonation energy (Q), velocity (D) and pressure (P), we have applied the Kamlet–Jacobs (K–J) empirical scheme.[53] The latter was recently found to be more accurate than the most recent predictors, like EMDB, EXPLO5 and Cheetah 8.0.[54] We should stress, however, that this empirical scheme performs well only for C–H–N–O compounds for which more experimental data are available. Meanwhile, for inorganic explosives (especially with heavy metals) or organic explosives, for which the K–J scheme is not calibrated, the above-specified software performs better. Thus, taking into account empirical formulas of salts **1–10**, the corresponding structural criteria are listed in Table 4. Within this approach, for the general empirical formula $C_aH_bN_cO_d$, the structure-derived dimensionless parameters N and $\bar{M}$ are calculated using eqn (7)–(9).[53]

$$N = (b + 2c + 2d)/4\mathrm{MW} \quad (7a)$$

$$N = (b + c)/2\mathrm{MW} \quad (7b)$$

$$\bar{M} = 4\mathrm{MW}/(b + 2c + 2d) \quad (8a)$$

$$\bar{M} = (2b + 28c + 32d)/(b + c) \quad (8b)$$

$$Q = (28.9b + 94.05a + 239\Delta H_f^0)/\mathrm{MW} \quad (9a)$$

$$Q = (57.8d + 239\Delta H_f^0)/\mathrm{MW} \quad (9b)$$

Table 3 The calculated enthalpies of formation and sublimation (kJ mol^{-1}) of salts **1–10**

Salt	ν_1	ΔH^0_{gas}	ΔH_{sub}	ΔH^0_{solid}
1	33.2	914.6	164.3	750.3
2	7.5	857.2	156.1	701.1
3	26.7	435.9	214.6	221.3
4	48.7	413.6	150.5	263.1
5	59.9	668.9	187.9	481.0
6	30.4	1787.0	367.7	1419.3
7	7.9	929.7	245.8	683.9
8	16.6	509.0	153.2	355.8
9	19.2	1012.9	239.4	773.5
10	30.1	598.9	200.4	398.5

Table 4 The calculated detonation properties along with nitrogen content (N), oxygen balance (Ω_{CO_2}) and crystal density (ρ)

Crystal	Formula	Structural criterion	N (wt%)	Ω_{CO_2} (%)	ρ (g cm^{-1})	Q (cal g^{-1})	D (km s^{-1})	P (GPa)
H_6N_6	H_6N_6	$b/2 > d$	93.3	−53.3	1.740	1166.5	9.78	41.6
Salt **1**	$CH_7N_{11}O_2$	$b/2 > d$	75.1	−27.3	1.905	1437.7	9.75	43.6
Salt **2**	H_7N_9	$b/2 > d$	94.7	−42.1	1.725	1258.8	9.66	40.3
Salt **3**	$H_7N_7O_3$	$b/2 > d$	64.0	−5.2	1.903	1478.0	10.06	46.4
Salt **4**	$H_8N_8O_4$	$d \geq 2a + b/2$	60.9	0.0	1.766	1597.3	9.61	40.5
Salt **5**	$H_7N_9O_4$	$d \geq 2a + b/2$	64.0	+4.1	1.862	1609.5	9.90	44.3
Salt **6**	$C_2H_{14}N_{20}O_2$	$b/2 > d$	80.0	−41.1	1.806	1298.5	9.36	38.9
Salt **7**	$CH_7N_{11}O_3$	$b/2 > d$	69.7	−18.1	1.855	1523.3	9.53	41.0
Salt **8**	$H_7N_7O_2$	$b/2 > d$	71.5	−17.5	1.808	1463.4	9.95	44.0
Salt **9**	H_7N_{11}	$b/2 > d$	95.6	−34.8	1.796	1147.3	9.53	40.2
Salt **10**	$CH_7N_9O_6$	$d \geq 2a + b/2$	52.3	+3.3	1.866	1624.0	9.72	42.8
DOTZ[a]	$H_4N_4O_2$	$d \geq 2a + b/2$	60.9	0.0	1.834	1945.5	10.36	48.2

[a] 1,4,2,3,5,6-Dioxatetrazinane.[36]

Herein, eqn (7a)–(9a) are applied to salts **4**, **5** and **10**, while eqn (7b)–(9b) are utilized for the other salts; MW stands for the molecular weight.

The calculated detonation parameters are listed in Table 4. As follows from the D and P values, all the studied salts are much more powerful energetic materials compared to conventional explosives (RDX, HMX, FOX-7, *etc.*).[55] Moreover, only ε-CL-20 and octanitrocubane (ONC) have the D and P values being close or slightly higher than those of salt **3**. We should stress, however, that ε-CL-20 is evaluated as the most powerful non-nuclear explosive known. To a large extent, this is due to its very high crystal density (2.044 g cm^{-3}), which is one of the highest densities among the organic molecular crystals known. Conversely, salt **3** is a carbon-free substance which decomposes to two absolutely safe and environmentally friendly products, H_2O and N_2. Similar but slightly lower detonation properties demonstrate other carbon-free salts **5** and **8** (Table 4). At the same time, oxygen-free salts **2** and **9** demonstrate slightly lower densities, which may be ascribed to the weaker hydrogen bonds formed.

It is interesting to estimate the properties of hexazinane and its salts as solid propellants. For this purpose, we have applied the NASA CEA code.[56] The latter requires new reactants to be defined in the form of NASA 9-coefficients as a result of simultaneous fit of the following three polynomials:[57]

$$\frac{C_p{}^0}{R} = a_1T^{-2} + a_2T^{-1} + a_3 + a_4T + a_5T^2 + a_6T^3 + a_7T^4 \quad (10)$$

$$\frac{H^0}{RT} = -a_1T^{-2} + a_2T^{-1} + \ln T + a_3 + a_4\frac{T}{2} + a_5\frac{T^2}{3} + a_6\frac{T^3}{4} + a_7\frac{T^4}{5} + \frac{a_8}{T} \quad (11)$$

$$\frac{S^0}{R} = -a_1\frac{T^{-2}}{2} - a_2T^{-1} + a_3\ln T + a_4T + a_5\frac{T^2}{2} + a_6\frac{T^3}{3} + a_7\frac{T^4}{4} + a_9 \quad (12)$$

The temperature dependence of C_p, H and S, obtained after the thermodynamic property calculations, is presented graphically in Fig. S9 in the ESI.† Using our previously described code i97creator[54] and the PAC99 routine,[56] these data were converted into the NASA 9-coefficients, which are listed in the ESI.†

Thus, the calculated propulsive properties in terms of the finite-area combustor (FAC) approximation[56] are listed in Table 5. These data include combustion chamber temperature (CCT), specific impulse (I_{sp}), vacuum specific impulse (I_{vac}) and characteristic velocity (c^*), which are calculated with various oxidant-to-fuel weight ratios (O/F). As follows from Table 5, all the compounds, both monopropellants and those in mixtures with O_2, possess a substantially higher I_{sp} than ε-CL-20 (272.6 s).[58] Additionally, due to the high nitrogen content (Table 4) and complete absence or low carbon content, when used as solid rocket propellants, hexazinane and its salts are expected to produce missile trails of low visibility.[59]

The decomposition schemes corresponding to the maximum propulsive performance are presented in Table S7† and the mole fractions of species formed upon

Table 5 The calculated propulsive properties of hexazinane and its salts with various O/F ratios at 300 K

Crystal	O/F	CCT (K)	I_{sp} (s)	I_{vac} (s)	c^*
H_6N_6	0	2440	286.9	302.4	1771.7
	0.2667	3023	310.8	334.8	1863.1
Salt **1**	0	2934	284.8	303.6	1727.6
	0.0975	3084	290.3	313.5	1737.4
Salt **2**	0	2690	292.6	309.3	1797.8
	0.2103	3085	307.0	331.4	1838.2
Salt **3**	0	2896	285.3	308.6	1704.5
Salt **4**	0	2919	283.1	308.9	1691.6
Salt **5**	0	3009	283.3	309.4	1692.2
Salt **6**	0	2674	276.0	291.9	1697.5
	0.2284	3108	293.3	318.1	1752.3
Salt **7**	0	3021	285.7	306.9	1717.1
	0.0724	3079	286.0	310.9	1707.6
Salt **8**	0	2904	295.3	316.6	1778.8
	0.0525	2967	296.8	320.4	1776.0
Salt **9**	0	2667	279.8	295.7	1720.6
	0.1986	3076	296.8	320.2	1776.3
Salt **10**	0	2998	273.6	299.9	1633.8

decomposition of the studied salts at various exit-to-throat ratios (Ae/At) of FAC are listed in Table S8 in the ESI.† Indeed, only salt **6** produces carbon soot (4 moles per 5 moles of salt) used as a monopropellant. The other materials produce only gaseous species (N_2, H_2, H_2O, CO and CO_2), among which only water vapor can be the reason for secondary smoke.[59] Meanwhile, the use of hexazinane or salts **2** and **9** as monopropellants allows avoiding of this drawback since the only exhaust gases are invisible N_2 and H_2. Moreover, salt **2** produces very high I_{sp} as a monopropellant (292.6 s).

Conclusions

In summary, we have presented in this paper a comprehensive theoretical evaluation of hexazinane and its most promising salts as energetic materials. The results clearly show hexazinane to be accessible in the crystalline state regardless of its conformation. Of course, hexazinane or similar compounds are not yet synthesized, but some efforts are already made towards the synthesis of H_xN_y compounds. Thus, at 10 GPa a linear $H_{10}N_{12}$ backbone is already synthesized; though, below 10 GPa, this material transforms into hydrazine.[60] We should stress that a similar situation was in the case of cg-N and *cyclo*-N_5^-, which took 12 and 15 years from prediction/observation to synthesis, respectively.[61–64] Moreover, in 2004, cg-N was obtained under extreme conditions (2000 K, 110 GPa), but encapsulation into a carbon nanotube in 2017 allowed obtaining of cg-N under near ambient conditions.[65] Thus, we believe experimentalists will find a synthetic route towards hexazinane and its salts in future.

Being a much stronger base than ammonia, hexazinane should easily form onium salts even with weak acids. Probably, the subsequent ion exchange reaction can be a route to a variety of its salts. Its high enthalpy of formation, good crystal density and high nitrogen content make hexazinane an excellent energetic material, which outperforms almost all the known non-nuclear explosives excluding ε-CL-20 and ONC. Meanwhile, the onium salts of hexazinane demonstrate even higher detonation and propulsive performance. For example, hexazinanium nitrate (salt **3**) has detonation properties which are comparable with those of ε-CL-20. Additionally, dinitramide (salt **5**) and nitrite (salt **8**) have only slightly lower characteristics, which make all these compounds one of the most powerful explosives that has ever been predicted. We should also point out that the carbon- and oxygen-free salts **2** and **9** may find practical application as solid rocket propellants which can produce invisible exhaust plumes.

Of course, an important issue which needs to be studied is the sensitivity of hexazinane and its salts, which is expected to be high. Unfortunately, a simple model for the calculation of the thermal stability of the hexazinane salts can scarcely be applied taking into account the complex decomposition pattern of similar ammonium salts (*e.g.*, NH_4NO_3);[68] this is the issue of a separate study. Recently, we have developed an approach for the prediction of impact sensitivity,[39,66] but a real crystal structure is crucial for such predictions,[67] since bulk modulus, crystal habits and other properties are strongly polymorph-dependent. However, it is known that the formation of salts leads to the decrease of impact sensitivity due to the more chemically hard species formed. Anyway, the further synthesis of hexazinane and its salts is very desirable and can shed light on this phenomenon.

Conflicts of interest

There are no conflicts to declare.

Acknowledgements

This work was supported by the Ministry of Education and Science of Ukraine, Research Fund (Grant No. 0118U003862).

Notes and references

1 J.-J. Fan, Y.-X. Tan, L.-C. Li, X. Wang, A.-M. Tian and N.-B. Wong, *J. Mol. Struct.: THEOCHEM*, 2008, **850**, 55–60.
2 J. Ledgard, *The Preparatory Manual of Explosives: Radical, Extreme, Experimental Explosives Chemistry*, ed. J. Ledgard, 2010, vol. 1, pp. 87–100.
3 Open chemistry database at the National Institutes of Health, (accessed Dec 26, 2019), https://pubchem.ncbi.nlm.nih.gov/.
4 First Chemical Database Based on Quantum Mechanics, (accessed Dec 26, 2019), https://www.molinstincts.com/.
5 W. Chi, B. Li and H. Wu, *Struct. Chem.*, 2013, **24**, 375–381.
6 R. Peverati, J. S. Siegel and K. K. Baldridge, *Phys. Chem. Chem. Phys.*, 2009, **11**, 2387–2395.
7 A. Karahodza, K. J. Knaus and D. W. Ball, *J. Mol. Struct.: THEOCHEM*, 2005, **732**, 47–53.
8 S. V. Bondarchuk, *Phys. Chem. Chem. Phys.*, 2019, **21**, 22930–22938.
9 H. Gao and J. M. Shreeve, *Chem. Rev.*, 2011, **111**, 7377–7436.
10 P. He, J.-G. Zhang, X. Yin, J.-T. Wu, L. Wu, Z.-N. Zhou and T.-L. Zhang, *Chem. – Eur. J.*, 2016, **22**, 7670–7685.
11 P. He, L. Wu, J. Wu, Q. Wang, Z. Li, M. Gozin and J. Zhang, *Chem. – Eur. J.*, 2017, **23**, 11159–11168.
12 Y. Liu, Y. Xu, Q. Sun and M. Lu, *CrystEngComm*, 2019, **21**, 6093–6099.
13 P. He, J. Liu, J. Wu, H. Mei and J. Zhang, *Chem. – Asian J.*, 2019, **14**, 3845–3849.
14 X.-H. Li, C. Zhang and X.-H. Ju, *RSC Adv.*, 2019, **9**, 26442–26449.
15 G. Zhao, D. Kumar, L. Hu and J. M. Shreeve, *ACS Appl. Energy Mater.*, 2019, **2**, 6919–6923.
16 Y. Xu, L. Tian, D. Li, P. Wang and M. Lu, *J. Mater. Chem. A*, 2019, **7**, 12468–12479.
17 C. Yang, C. Zhang, Z. Zheng, C. Jiang, J. Luo, Y. Du, B. Hu, C. Sun and K. O. Christe, *J. Am. Chem. Soc.*, 2018, **140**, 16488–16494.
18 R. Gilardi and R. J. Butcher, *J. Chem. Crystallogr.*, 2000, **30**, 599–604.
19 J. C. Bottaro, P. E. Penwell and R. J. Schmitt, *J. Am. Chem. Soc.*, 1997, **119**, 9405–9410.

20 W. L. Masterton, E. J. Slowinski and C. L. Stanitski, *Chemical principles*, CBS College Publishing, Philadelphia, 1983.
21 A. R. Oganov and C. W. Glass, *J. Chem. Phys.*, 2006, **124**, 244704.
22 B. A. Steele and I. I. Oleynik, *J. Phys. Chem. A*, 2017, **121**, 1808–1813.
23 R. L. C. Akkermans, N. A. Spenley and S. H. Robertson, *Mol. Simul.*, 2013, **39**, 1153–1164.
24 Q. Zhu, A. R. Oganov, C. W. Glass and H. T. Stokes, *Acta Crystallogr., Sect. B: Struct. Sci.*, 2012, **68**, 215–226.
25 T. Frauenheim, G. Seifert, M. Elstner, T. Niehaus, C. Köhler, M. Amkreutz, M. Sternberg, Z. Hajnal, A. Di Carlo and S. Suhai, *J. Phys.: Condens. Matter*, 2002, **14**, 3015–3047.
26 M. Gaus, A. Goez and M. Elstner, *J. Chem. Theory Comput.*, 2013, **9**, 338–354.
27 A. D. Becke, *J. Chem. Phys.*, 1993, **98**, 5648–5652.
28 W. J. Hehre, L. Radom, P. V. R. Schleyer and J. A. Pople, *Ab Initio Molecular Orbital Theory*, Wiley, New York, 1986.
29 M. J. Frisch, G. W. Trucks, H. B. Schlegel, G. E. Scuseria, M. A. Robb, J. R. Cheeseman, G. Scalmani, V. Barone, B. Mennucci and G. A. Petersson, *et al.*, *Gaussian 09, Revision A.02*, Gaussian, Inc., Wallingford, CT, 2009.
30 H. Sun, *J. Phys. Chem. B*, 1998, **102**, 7338–7364.
31 S. J. Clark, M. D. Segall, C. J. Pickard, P. J. Hasnip, M. J. Probert, K. Refson and M. C. Payne, *Z. Kristallogr. – Cryst. Mater.*, 2005, **220**, 567–570.
32 *Materials Studio 7.0*, Accelrys, Inc., San Diego, CA, 2013.
33 J. P. Perdew, K. Burke and M. Ernzerhof, *Phys. Rev. Lett.*, 1996, **77**, 3865–3868.
34 S. Grimme, *J. Comput. Chem.*, 2006, **27**, 1787–1799.
35 B. Delley, *J. Chem. Phys.*, 2000, **113**, 7756–7764.
36 S. V. Bondarchuk, *J. Phys. Chem. Solids*, 2020, **142**, 109458.
37 S. V. Bondarchuk, *Polymer*, 2020, **186**, 122048.
38 P. Hartman and P. Bennema, *J. Cryst. Growth*, 1980, **49**, 145–156.
39 S. V. Bondarchuk, *CrystEngComm*, 2018, **20**, 5718–5725.
40 N. Liu, Y.-N. Li, S. Zeman, Y.-J. Shu, B.-Z. Wang, Y.-S. Zhou, Q.-L. Zhao and W.-L. Wang, *CrystEngComm*, 2016, **18**, 2843–2851.
41 F. Mouhat and F.-X. Coudert, *Phys. Rev. B: Condens. Matter Mater. Phys.*, 2014, **90**, 224104.
42 W. Setyawan and S. Curtarolo, *Comput. Mater. Sci.*, 2010, **49**, 299–312.
43 P. K. Chattaraj, U. Sarkar and D. Ranjan Roy, *Chem. Rev.*, 2006, **106**, 2065–2091.
44 L. R. Domingo and P. Pérez, *Org. Biomol. Chem.*, 2011, **9**, 7168–7175.
45 NIST Chemistry WebBook, (accessed Dec 26, 2019), https://webbook.nist.gov/chemistry/.
46 M. R. Manaa, I.-F. Kuo and L. E. Fried, *J. Chem. Phys.*, 2014, **141**, 064702.
47 T. M. Klapötke, *Chemistry of High-Energy Materials*, De Gruyter, Berlin, 3rd edn, 2015, p. 319.
48 V. P. Sinditskii, S. A. Filatov, V. I. Kolesov, K. O. Kapranov and A. O. Suprun, *Combustion and Explosion*, 2015, **8**, 186–194.
49 CSD Space Group Statistics – Space Group Number Ordering 2019, (accessed Dec 26, 2019), https://www.ccdc.cam.ac.uk/.
50 C. P. Brock and J. D. Dunitz, *Chem. Mater.*, 1994, **6**, 1118–1127.
51 J. Nyman and G. M. Day, *CrystEngComm*, 2015, **17**, 5154–5165.
52 S. V. Bondarchuk, *J. Mol. Graphics Modell.*, 2019, **89**, 114–121.
53 M. J. Kamlet and S. J. Jacobs, *J. Chem. Phys.*, 1968, **48**, 23–35.
54 S. V. Bondarchuk and N. A. Yefimenko, *Propellants, Explos., Pyrotech.*, 2018, **43**, 818–824.
55 H. H. Krause, New Energetic Materials, in *Energetic Materials: Particle Processing and Characterization*, ed. U. Teipel, WILEY-VCH, Weinheim, 2005, p. 621.
56 S. Gordon and B. J. McBride, *Computer program for calculation of complex chemical equilibrium compositions and applications. I. Analysis, NASA Reference Publication 1311*, NASA, Cleveland, OH, 1994.
57 A. Burcat, Thermochemical Data for Combustion Calculations, in *Combustion Chemistry*, ed. W. C. Gardiner Jr, Springer, Berlin, 1984, pp. 455–473.
58 R. D. Chapman, Organic Difluoramine Derivatives, in *High Energy Density Materials*, ed. T. M. Klapötke, Springer, Berlin, 2007, vol. 125, pp. 123–151.
59 G. P. Sutton and O. Biblarz, *Rocket Propulsion Elements*, John Wiley & Sons, Inc., Hoboken, 9th edn, 2017, p. 767.
60 H. Wang, M. I. Eremets, I. Troyan, H. Liu, Y. Ma and L. Vereecken, *Sci. Rep.*, 2015, **5**, 13239.
61 C. Mailhiot, L. H. Yang and A. K. McMahan, *Phys. Rev. B: Condens. Matter Mater. Phys.*, 1992, **46**, 14419–14435.
62 A. Vij, J. G. Pavlovich, W. Wilson, V. Vij and K. O. Christe, *Angew. Chem., Int. Ed.*, 2002, **41**, 3051–3054.
63 M. I. Eremets, A. G. Gavriliuk, I. A. Trojan, D. A. Dzivenko and R. Boehler, *Nat. Mater.*, 2004, **3**, 558–563.
64 C. Zhang, C. G. Sun, B. C. Hu, C. M. Yu and M. Lu, *Science*, 2017, **355**, 374–376.
65 E. M. Benchafia, Z. Yao, G. Yuan, T. Chou, H. Piao, X. Wang and Z. Iqbal, *Nat. Commun.*, 2017, **8**, 930.
66 S. V. Bondarchuk, *J. Phys. Chem. A*, 2018, **122**, 5455–5463.
67 S. V. Bondarchuk, *New J. Chem.*, 2019, **43**, 1459–1468.
68 S. Cagnina, P. Rotureau, G. Fayet and C. Adamo, *Phys. Chem. Chem. Phys.*, 2013, **15**, 10849–10858.